

Dodging the crisis of folding proteins with knots

Joanna I. Sułkowska^{1,2}, Piotr Sułkowski^{3,4}, José N. Onuchic¹

¹*Center for Theoretical Biological Physics, University of California San Diego,
Gilman Drive 9500, La Jolla 92037*

²*Institute of Physics, Polish Academy of Sciences,
Al. Lotników 32/46, 02-668 Warsaw, Poland*

³*Physikalisches Institut der Universität Bonn and Bethe Center for Theoretical Physics,
Nussallee 12, 53115 Bonn, Germany*

⁴*Soltan Institute for Nuclear Studies, Hoza 69, 00-681 Warsaw, Poland*

Abstract

Proteins with nontrivial topology, containing knots and slipknots, have the ability to fold to their native states without any additional external forces invoked. A mechanism is suggested for folding of these proteins, such as YibK and YbeA, which involves an intermediate configuration with a slipknot. It elucidates the role of topological barriers and backtracking during the folding event. It also illustrates that native contacts are sufficient to guarantee folding in around 1-2% of the simulations, and how slipknot intermediates are needed to reduce the topological bottlenecks. As expected, simulations of proteins with similar structure but with knot removed fold much more efficiently, clearly demonstrating the origin of these topological barriers. Although these studies are based on a simple coarse-grained model, they are already able to extract some of the underlying principles governing folding in such complex topologies.

knots | slipknots | proteins | folding | backtracking | molecular dynamics

During the last two decades, a joint theoretical and experimental effort has largely advanced the quantitative understanding of the protein folding mechanism. Most small and intermediate size proteins live on a minimally frustrated funnel-like energy landscape, which allows fast and robust folding [1, 2, 3]. Since proteins have been able to solve the energy problem, the final challenge is the structural complexity of the protein folding motifs. Most proteins avoid complex topologies, but recent discoveries have shown that some proteins are actually able to fold into non-trivial topologies where the main chain folds into a knotted conformation [4, 5, 6]. Although these “knotted” folding motifs have been observed, we still have to face the challenging question of how the protein overcomes the kinetic barrier associated with the search of the knotted conformation. We suggest a possible mechanism where the knot formation is preceded by a conformation called a “slipknot”. A slipknot is topologically similar to a knot, except that an internal knot is effectively undone as the pathway of the backbone folds back upon itself. The fact that such slipknots have already been observed in some protein final structures [7] adds support to this suggestion.

This folding mechanism is explored in the context of the two most experimentally investigated knotted families of proteins, *Haemophilus influenzae* YibK and *Escherichia coli* YbeA, which are homodimeric β -knot methyltransferases (MTases). A schematic representation of these proteins is shown in Fig. 1. It has been shown experimentally that both these proteins unfold spontaneously and reversibly upon addition of chemical denaturant [9, 8, 10, 11] and they are able to fold even when additional domains are attached to one or both termini [12]. In very recent experimental work [13], based on analysis of the effect of mutations in the knotted region of the protein, a folding model for YibK was also proposed. In this model the threading of the polypeptide chain and formation of the native structure in the knotted region can occur independently as successive events. These results alone, though, are not sufficient to explain the folding mechanism. To complement the experimental information, we have devised a theoretical computational strategy. Simulations are performed for three proteins using structure-based coarse-grained models, based on the β -knot superfamily YibK and YbeA.

In the present study we consider knots of simplest type, referred to as a trefoil or 3_1 knot. It that consists of a loop through which one end of a chain is threaded. In principle there might be three possible mechanisms leading to the creation of such a knot. The most straightforward one would require just two steps: creating a loop and threading one end through it. The second mechanism is more complicated and involves an intermediate step with a slipknot. The third and final possibility would involve the creation of an ensemble of loose random knots in the first stage, which may turn into deeper knots after a relatively longer time. Analysis of simulated folding trajectories provides the necessary insight on this complex folding event. The results indicate that the folding of YibK and YbeA proceeds according to the second mechanism, through a slipknot intermediate configuration. This is consistent with earlier theoretical observations [6, 7]. Fig. 2 provides a detailed description

of the suggested folding mechanism.

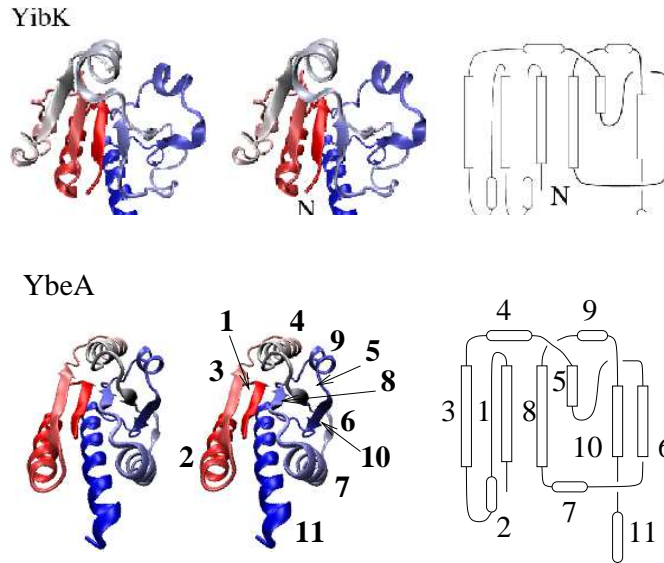


Figure 1: Structure of knotted proteins. Top panel – stereo view of structure of knotted protein YibK (1j85) (left) and its schematic structure (right). Bottom panel – stereoview of YbeA (1od6) and its schematic structure (left). Details of proteins structure are described in *Appendix*.

Understanding the folding mechanism for these knotted proteins provides the tools to explore additional complex folds. For example, one can extend these studies to proteins that do not fully knot but form a slipknot in the native state. Some slipknotted proteins have a simple folding motif such as crenarchaeal viruses AFV3-109 [17] but others, such as thymidine kinase [16], are longer and have a more complex folding mechanism.

1 Results - Folding Knotted Proteins

The folding pathways which lead to the knotted conformation are observed in our simulations through an intermediate configuration containing a slipknot. This route is shown schematically in Fig. 2 and discussed below. Analysis of this suggested folding mechanism requires that we divide this route into a few geometrically distinctive steps. A step may consist, for example, of threading the chain through a loop created in a separate region of the sequence. This representation allows us to describe long folding trajectories, consisting of thousands steps in our simulations, by a sequence of the essential intermediate ensemble of configurations. When projected on a plane, certain transitions between such two adjacent configurations can be identified with so called Reidemeister moves. The Reidemeister moves change a relative location of some strands (when projected on a plane),

but do not change the type of the knot. There are three such moves, denoted I, II and III, that involve respectively one, two and three strands. They are described in detail in *Appendix*.

1.1 Folding proteins in the 3_1 -knot superfamily into a trefoil knot

Our analysis is based on the simulations of the 3_1 -knotted proteins YibK (PDB code 1j85) and YbeA (PDB code 1o6d, 1vho), shown in Fig. 1, which are homodimers in their native configuration. According to the experimental results [8, 10] they fold via a few intermediate steps reaching the stable monomer states with considerable structure. Only the last step involves formation of a dimer. This allows us to study these proteins as monomers. Notice that YibK shares only 19% sequence identity with YbeA [10]. Folding simulations were performed at temperatures slightly above the folding temperature T_f , starting from random conformations. Simulations were run utilizing a standard C structure-based model (sometimes called Go Model) [18, 19]. For each protein (1j85, 1o6d, and 1vho) we observed at least 10 successful folding trajectories; around 1-2% of all routes succeeded to reach the native knotted states. These successful trajectories choose between two parallel folding trajectories similarly to what has been proposed experimentally [8, 10]. Both trajectories are characterized by an intermediate slipknot configuration but in one case it is formed early in the folding process while, in the other one, it is a late event. Fig. S2 in *Appendix* shows the fraction of native contacts Q at the moment when the slipknot is being created, i.e. when its hook-region starts to be threaded through the loop 66-96. In the most common trajectory the structure elements located closer to the N terminal of the protein fold in the final stages of the folding process around $Q \approx 0.8$. In the alternative trajectory, the N terminal folds in the early stages of folding, thus when the slipknot is being created $Q \approx 0.6$. In fact there is also an additional but very rare possibility (which we observed only once) of formation a knot by threading the terminus C through the loop 66-96 without a slipknot intermediate.

For clarity we now discuss in detail one folding trajectory for 1o6d, shown schematically in Fig. 2 (this is the smallest of all proteins being analyzed and therefore had the largest number of successful runs). Although we focus on this single example, this trajectory is similar to other proteins with a knot 3_1 , as 1vho, 1j85. This folding route consists of six distinctive intermediate configurations. During the first transition a loop is created (the Reidemeister move I). This loop extends between amino acids 66 and 96 and remains formed during the entire folding event. Following this step, a further region of the chain gets close to the loop, requiring a hook formation (the Reidemeister move II). This hook is then threaded through the loop (also move II), creating the slipknot in the fourth intermediate. The slipknot is then transformed into a knot by pulling one termini through the loop, which may be viewed as a two-step process, with an intermediate 5 and final configuration 6. There are no Reidemeister moves corresponding to these last two steps, because they

could not happen for a closed chain without cutting it.

As argued above, the creation of a knot requires several turns to occur at the right place and at the right time order. In the trajectory shown in Fig. 2 these turns are represented by grey dots. The first one occurs at amino acid 102, which redirects the protein chain towards the loop 66-96. Then two other turns at positions 114 and 125 are needed for the hook formation. This hook is threaded through the loop 66-96. Finally the termini 147 is pulled through this loop which results in the 3_1 knot.

To understand the knot formation, we investigate the order that native contacts are formed and, sometimes, broken and reformed (backtracking) during the folding event. Correlation between formation of some native contacts with the backtracking of other ones can teach us about topological bottlenecks. This information can be extracted from Fig. 3, where the time dependence of the number of formed native contacts between relevant structural elements of the protein knot is shown. Initially we focus on the formation of the loop between residues 66 and 96 that requires the creation of contacts between α -strands 5 and 8. This can only be achieved by the pre-formation of the contacts between 5 and 10, which is followed by a simultaneous destruction of these contacts and formation of the ones between 5 and 8. During this loop formation, contacts between strands 6 and 10 are also formed, which are needed to create the slipknot conformation. The formation and destruction (around 180 timesteps) of contacts between strands 5 and 10 is an example of backtracking. Backtracking also plays a role in the formation of contacts between 5 and 9 and between 6 and 9. The order of contact formation is crucial, otherwise knotting is not possible.

Backtracking is also a mechanism to escape from kinetic traps as described in Fig. 2. For example, if 8-11 contacts are formed early, the creation of a loop between residues 66 and 96 becomes impossible. The 8-11 contacts need to be broken before this loop can be created. A similar situation occurs at the final stage of knot creation that involves threading the helix 11 through the loop. During this process, contacts between helices 7 and 11 may be accidentally created. They need to be broken until further threading can proceed.

1.2 Energetic heterogeneity enhancing folding ability

The results above demonstrate that making only the native contacts attractive is sufficient to fold the protein into its native conformation. The percentage of successful trajectories, however, is then very small – only about 0.1%. Analysis of this data suggests that this success rate can be increased by improving the time-order of contacts formation and therefore reducing backtracking. We utilized different strength for a few selected native interactions to achieve this folding improvement. Backtracking gets reduced but the overall folding mechanism remains the same as described in Fig. 2.

Guided by the results of Fig. 3 which identifies the structural regions responsible for

enhancing folding, we modified some of our contact interactions. We increased the strength of contacts between strands 5 and 8. This modification facilitates the formation of the loop between residues 66 and 96 and also the attachment of the C terminal to this loop, which leads to the slipknot conformation involving the contacts between strands 6 and 10. We also slightly reduced the interaction energy between the C-terminal and the loop. Rapid formation of those contacts results in problematically fast blocking of the necessary backtracking and threading of the C-terminal across the loop. Simulations with this "optimal" model succeeded in folding into the knotted structure 29 times in 2500 trials. Further increasing the contact strength in these regions does not keep improving knot formation. Since backtracking is also needed during the knotting process, if those increases are too large, they will lead to more kinetic traps. For further analysis on how this "optimal" set of contacts have been determined see the *Appendix*.

1.3 Extension of the protein chain and a rebuilt protein without knot structure

We also analyzed how folding properties of these proteins were affected when additional chains (tails) were attached to one or both termini following the idea of experiments reported in [12]. Due to computational limitations we restricted our studies to purely flexible homopolymer tails built of no more than 12 residues.

The addition of these tails not only did not restrict, but sometimes even increased the number of correctly formed knotted native states. The last step in the folding process, which involves pulling the entire tail through the loop, is slower than in the regular protein. Nonetheless, the overall folding time is similar in both cases.

The final test which can clarify the folding ability of the knotted protein (1j85) and the presence of a topological barrier is to use a modified protein in which the knot is absent. To engineer such a protein with a trivial topology, it is sufficient to change the crossing of protein chain between 78-85 and 120-125 amino acids using methods from [14, 15]. The folding ability of such an untightened structure increases to a 73% success for equally long folding runs. This means that a simple change of topology eliminates an otherwise very high topological barrier.

2 Results - Folding Proteins with Slipknots

So far we have discussed proteins that have a 3_1 knot in the native conformation. Our suggested folding mechanism via a slipknot intermediate configuration gets further support from the fact that in a different class, proteins actually contain slipknots in their native states [6, 7]. Comparing their folding mechanism to our initial results provides further understanding of our proposed model. We focus on a relatively short protein 2j6b (consisting of 109 amino acids) and a much longer one 1p6x (333 amino acids), which

are shown in Fig. 4. Again, a model that includes only attractive interactions for native contacts is sufficient to fold these proteins. Although both these proteins contain slipknots, their folding trajectories are different. Folding of 2j6b is composed simply by the first three steps in Fig. 2. This independently provides strong support for our proposed folding mechanism for the knotted proteins. Formation of a slipknot in 1p6x is more complicated and it is described below.

The folding mechanism for the short protein 2j6b involves creation of a loop through which a hook is subsequently threaded. As discussed above, its folding is analogous to the first three steps of folding of 1o6d. Again, folding simulations were run at temperatures slightly above T_f . Based on 1000 trajectories, we found four different ensembles of final conformations, shown in Fig. 5. Only 2.8% of these trajectories reached the correct folding basin using three slightly different routes. A few conformations (0.5%) in the "OTHER" basin in Fig. 5 have most of the native contacts formed but do not form the slipknot. Interestingly, the typical folding time for these trajectories is much longer than for such ones that reach the correct native folding. This indicates that slipknot creation should be a fast process, as long as the correct trajectory is followed. We have also attached a tail to 2j6b to the termini which is closer to the slipknot conformation. Similarly to the knotted proteins, it did not substantially affect its folding properties. These extended proteins were able to fold into slipknot configurations in a similar fashion to the original protein.

We now discuss thymidine kinase (PDB code 1p6x), whose structure is described in detail in the *Materials and Methods* section. We checked its folding ability at several temperatures above T_f , and for each one we ran 500 trajectories. The highest probability of folding was observed at temperatures 18% above T_f . In a set of 8000 trajectories, the correctly folded conformation including the slipknot and all native contacts was reached only 11 times. In an additional 12 cases, the slipknot was created but in a structure with an incorrectly folded bundle of 5 helices; in these cases 92% of native contacts were established. In yet another set of 13 trajectories, although most of the native contacts were formed, a knot instead of a slipknot was observed in the final structure. Knotted structures were reached in 5-20% of the runs at each temperature and they had typically less than 73% of native contacts. All other final structures were some trivial kinetic traps or misfolded conformations.

Folding of the 1p6x protein, due to its large size and complexity, is more interesting than folding of the previously discussed proteins. It can start from several nucleation sites. One of such sites includes a loop similar to the one reached after the first step in Fig. 2. Notice that in the folding motif both termini are close to the loop. Also, during folding, both of them have to cross the loop. This implies that, even though in the folding of 1p6x the steps from Fig. 2 are used, it proceeds in a different way than creation of a slipknot in 1o6d (where only one terminus had to be threaded through a similar loop). Therefore the folding mechanism is similar to the one shown in Fig. 2 but then the second terminus also has to thread through the loop.

For the 11 correctly folded trajectories, we identified four possible folding routes [19]. They were classified according to the instant during folding in which the slipknot contacts are formed for the first time (see Fig. 11). Three of these four possible routes, albeit slightly different, have basically the folding mechanism described in Fig. 2 plus an additional step. As before their folding mechanism leads initially to the knot formation close to the N terminal. This is followed by threading the C terminal through the loop. This final step gives rise to the slipknot conformation. These three folding routes share several common features. First, their nucleation sites, although they always include the loop, are composed by different additional regions of the protein [20]): bundles of alpha helices, a vicinity of the helix at the N terminal, or a huge loop close to the C terminal. Second, both termini enter the loop in configuration of a loosely packed hairpin. Third, for all folding trajectories, backtracking is related to two topological barriers associated with the formation of the knot closest to the N terminal and to the slipknot formation during last stages of folding.

The fourth folding route is different from the ones mentioned above. Similarly to the previous cases, this route involves a creation of a knot close to N terminal and a slipknot that involves terminal C. At the late stages of folding however it also requires a huge rotation of the knotting loop (denoted by loop 4 in Fig. 6). Both the knot and the slipknot are formed almost simultaneously during this surprising rotation of loop 4 by almost 360 degrees, as shown by three steps in Fig. 6. This one move makes the protein structure non-trivial. It has to be pointed out that some deviations of this route are also possible, but a critical role is always played by rotation of loop 4. More details about the trajectories described above are given in the *Appendix*. We suggest that this mechanism, involving a rotation of the loop together with the steps from figure 2, should be typical in folding bigger and more complicated knotted structures.

3 Discussion and conclusions

The analysis of folding trajectories for topologically nontrivial proteins allows us to explore possible mechanisms for creation of knots and slipknots. Furthermore the results emphasize difficulties associated with these processes that commonly lead to kinetic traps. Below we summarize these two issues.

3.1 Folding mechanism for nontrivial topologies

Folding into topologically nontrivial configurations is associated to a series of complex events. Transitions between different stages in this process are nontrivial. In many cases they are not successful, which is associated with a presence of so called **topological barriers**. When a protein does not manage to overcome such a barrier, it may be captured into an improper configuration – a **kinetic trap**. Even successful events that overcome such a barrier may require a series of partial unfolding and refolding events, which we

call a **backtracking**. Since backtracking is a stochastic process, it may lead to a broad distribution of time scales for such transitions.

The proteins YibK (1j85) and YbeA (1o6d, 1vho) have the simplest type of knot, 3_1 . We determined that, in most cases, folding into this knotted structure goes through **an intermediate configuration which contains a slipknot**, Fig. 2. A presence of this slipknot was conjectured in [6, 7], and our results confirm this prediction. A slipknot arises after threading a partially structured region, which we call a **hook**, through a previously created **loop**. The appearance of an intermediate slipknot in our simulations also suggests a plausible mechanism for the creation of deep knots (located far from both termini). We also expect that more complicated types of knots (such as 4_1 and 5_2 [5]) are formed through a similar intermediate slipknot configuration. Supporting this suggestion is the fact that the native state of ubiquitin hydrolase UCH-L1 (PDB code 2etl) contains a sharp turn close to its C terminus, which might be a remnant of an intermediate slipknot.

Folding into knots and slipknots involves precise geometrical constraints. Knots and slipknots require threading a region of the protein through a loop. Protein chains, however, are not flexible strings since they are composed of helices and β -strands that typically do not freely bend. Since creation of a tight knot requires **sharp turns**, the protein needs to have properly located regions that allow for bending and motion. Locations of such regions cannot be accidental. For example, these sharp turns should occur around the loop region to facilitate threading. As shown in Fig. 2, loop formation has to precede a sharp turn, otherwise correct loop formation would be impossible and would lead to kinetic trapping. Careful analysis of the protein structure already allows us to identify these bend regions before simulations are performed.

3.2 Topological barriers and kinetic traps

We suggest that the folding mechanism in Fig. 2 provides a route that reduces the topological barriers in the free energy landscape of knotted proteins. These topological barriers have already been proposed earlier from an analysis of the structure (topology) of various proteins [20]. In our folding studies, these topological constraints due to the presence of knots severely restrict possible folding routes. Topological constraints strongly restrict the folding landscape [2, 3] and only allow one or a few similar trajectories leading to the native state. An improper step along each such pathway may lead to a kinetic trap, which corresponds to a local minimum in the folding landscape. For shallow traps, the protein can resolve this kinetic problem with the aid of backtracking.

Our numerical analysis has identified various types of kinetic traps. Recall that the geometry of a knot or a slipknot requires the formation of sharp turns or flexible regions in appropriate places. These sharp turns often arise on prolines or glycyines. Turns at amino acids 102, 114 and 125 in 1o6d in Fig. 2 exemplify these regions. Turns are also formed at amino acids Pro and Gly (number 62 and 63) in the native conformation. These are

late turns formed much later than the others during the folding event. During folding, however, these turns may be formed in an incorrect time order and/or may be formed at additional prolines or glycines. In this situation the protein is unable to fold in the correct conformation. For example, when the turn at position 62 and 63 in 1o6d is formed too early, it precludes the correct route towards folding.

The simple appearance of an intermediate configuration with a slipknot during the folding event does not yet guarantee that it will be followed by the formation of a knot. The hook, which is required to move into the previously formed loop, may turn back and leave the loop, as shown in the fourth step of Fig. 2. Successfully crossing of the loop by the terminus is needed to overcome the topological barrier and therefore form the correct knot. Although we have successfully folded these proteins several times, these multiple geometrical requirements are difficult to satisfy, and lead to kinetic traps on many occasions, particularly if the simulation temperature is too low. These challenges have inspired others to propose alternative mechanisms to facilitate folding such as placing attractive long range non-native contacts [22] or chaperones to help push the hook through the loop. We submit that the use of non-native contacts prevents the crucial formation of an intermediate slipknot conformation. Our studies have the advantage of being based only on interactions associated to native contacts. This allows to observe and to understand the role of an intermediate slipknot in an unbiased way. Nonetheless, physically-motivated properly place non-native contacts, which do not interrupt the slipknot formation, may improve the success rate of folding events. This point is worth further study.

To further understand the effect of the knot, we rebuilt protein 1o6d into a very similar structure, but without knot topology [23]. As expected, under similar simulation conditions, the number of successful folding events increases substantially to about 83%. This shows that knot formation is the main limitation for folding, since in both cases the amino acid sequence is very similar, but the folding success rate is remarkably different. This provides direct evidence that the topological barrier arises as a consequence of knot formation.

Contrary to some previous experimental suggestions [12] that knot formation is preceded by a formation of random knots, we do not observe such a mechanism. Indeed, the analysis of protein conformations during early stages of folding clearly shows a noticeable number of randomly knotted structures. Such behavior agrees with results of simulations in [24] and well-known experimental results that flexible polymers or strings [25] can easily become spontaneously knotted. But in most cases random knots observed in folding simulations do not lead to deep but relaxed knots. Notice that at room temperature knots on a protein chain do not necessarily behave in the same way as in a polymer chain, which was shown in the case of stretching simulations [26]. Additionally our results show that the knotting mechanism is not prevented even when additional tails are attached to the protein, which was also observed in experiment [12]. Without an intermediate slipknot it would be hard to explain the creation of knots in this case. These results further support

the mechanism described in this paper.

Finally, it would be more satisfying to achieve a higher success rate of folding than just 1-2% in our simulations. Such a small success rate may be a consequence of several factors. Our folding routes may be too short. Some preliminary results indicate a higher degree of success for simulations five times longer. Also the simplicity of the model that includes only native interactions and no geometrical details may cause limitations. Even with these limited coarse-grained models, however, we have already been able to provide strong insights about the possible mechanism governing folding in knotted proteins that can now be checked by experiments and more detailed/expensive simulations.

4 Materials

4.1 Proteins with knots and slipknots studied

Knots observed in proteins are "open" knots, and so they differ from the mathematical definition of (closed) knots. Nonetheless, when both termini of the protein are located far enough from its entangled core, they usually can be unambiguously joined by an additional interval which transforms them to a closed loop. If such a loop is not homeomorphic to a circle then the native protein is regarded as representing a nontrivial (open) knot. The families of proteins with a trefoil knot 3_1 studied here are YibK (PDB code 1j85) and YbeA (including structures with PDB code 1o6d, 1vho). The slipknots are topological configurations more subtle than knots. They exist when a piece of a protein chain gets in and out of a loop formed by some other part of the chain. This means that cutting several residues from one end of the protein would lead to a configuration with an (open) knot, which is absent in the native state. One protein with a slipknot which we study is a highly conserved protein from crenarchaeal viruses AFV3-109 [17] (PDB code 2j6b). It consists of $N=109$ amino acids, belongs to α class and is built of five β strands, which form the sheet surrounded by a loop from one side and the helices on the other side, Fig. 4. This protein forms a dimer with the shape of a cradle [17]. 2j6b contains a slipknot, such that removing 9 amino acids from C terminal side leads to a knotted configuration. The smooth topological representations of 2j6b is shown in Fig. 4. The function of 2j6b is still unknown, however it was suggested that it could interact with nucleic acids [17]. The second protein with a slipknot which we study is a thymidine kinase [16] (PDB code 1p6x) which belongs to α class, consists of β sheet of 5 beta strands which are surrounded by 6 helices, and a bundle of 5 peripheral β helices, Fig. 4. It contains a slipknot, such that considering only amino acids 26-140 one finds a knot 3_1 made of 3 sheets and 3 helices. The slipknot arises when the bundle of helices and 2 sheets come back to the structure by the loop between 121 and 132 amino acids. As was described in [7] the slipknot is very deep on C terminal side, however it is shallow on the N terminal side, with only 10 residues extending out of the knot core. This difference suggests that

the knot is most likely formed by the N terminal segment of the protein passing through a loop in the protein arising during the later stages of the protein folding. Because the N terminal is shorter, the slipknot in thymidine kinase is considerably more shallow than the one in alkaline phosphatase; this knot is also much tighter. We use thymidine kinase to analyze its folding ability and mechanical properties. The analysis of protein structure is described in *Appendix*.

4.2 Reidemeister moves

Three Reidemeister moves shown in Fig. 11 describe basic geometric transformations which do not change a type of a knot. They are very useful in a simplified description of proteins with nontrivial topology.

4.3 Coarse-grained model

We use the coarse-grained molecular dynamics modeling described in detail in refs. [19, 27, 28]. The native contacts between the C atoms in amino acids i and j separated by the distance r_{ij} are described by the Lennard-Jones potential $V_{LJ} = 4 \left(\frac{\sigma_{ij}}{r_{ij}} \right)^{12} - \left(\frac{\sigma_{ij}}{r_{ij}} \right)^6$. The length parameter σ_{ij} is determined pair-by-pair so that the minimum in the potential corresponds to the native distance. The energy parameter ϵ is taken to be uniform. As discussed in ref. [30], other choices for the energy scale and the form of the potential are either comparable or worse when tested against experimental data on stretching. Implicit solvent features come through the velocity dependent damping and Langevin thermal fluctuation in the force. We consider the over-damped situation which makes the characteristic time scale, τ , to be controlled by diffusion and not by ballistic-motion, making it of order of a ns [34]. Thermodynamic stability of a protein can be characterized by providing the folding temperature T_f at which half of the native bonds are established on average in an equilibrium run (based on at least ten long trajectories that start in the native state). The analysis of the knot-related characteristics is made along the lines described in ref. [26].

4.4 KMT algorithm

We determine the sequential extension of a knot, i.e. the minimal segment of amino acids that can be identified as a knot, by using KMT algorithm [33]. It involves removing the C atoms one by one, as long as the backbone does not intersect a triangle set by the atom under consideration and its two nearest sequential neighbors.

5 Appendix

In this Appendix we present more details concerning the geometry and properties of knotted proteins (1j85, 1o6d and 1vho) and proteins with slipknots (2j6b and 1p6x). We present the Reidemeister moves necessary for a description of knot creation and describe attached video clips. Furthermore, we provide quantitative details of the fraction of native contacts, as well as the "optimal" energetic map which we found. Finally we describe in detail four folding trajectories of 1p6x.

A Proteins with knots and slipknots

A.1 Knotted proteins

Monomeric subunits of haemophilus influenzae YibK (PDB code 1j85) and escherichia coli YbeA (PDB codes 1o6d and 1vho) are shown in Fig. 7, together with schematic diagrams representing their topology. Another member of the methyltransferase YibK, the protein sr145 from Bacillus subtilis (1PDB code 1to0), is not suitable for our analysis as its chain is broken in many places.

Methyltransferase (Mtases) from Hamophilus influenzae YibK is described in detail in [10, 11].

Homodimeric α -knot methyltransferase (Mtases) from escherichia coli YbeA (1o6d), consists of 5 helices which surround the sheet built of 6 strands. The secondary structure elements are referred to as follow: 1 – strand (amino acids 2-8); 2 – helix (12-27); 3 – strand (31-37); 4 – helix (44-58); 5 – strand (65-69); 6 – strand (74-75); 7 – helix (77-92); 8 – strand (95-99); 9 – helix (106-113); 10 – strand (115-118); 11 – helix (125-145). The structure is knotted between strands 5 and 10.

The second protein from the YbeA family (1vho) has almost the same structure as 1o6d, however it is longer by 10 amino acids. It consists of 5 helices which surround the sheet built of 6 strands.

A.2 Proteins with slipknots

We analyse two proteins with slipknots: thymidine kinase [16] (PDB code 1p6x) and highly conserved protein from crenarchaeal viruses AFV3-109 [17] (PBD code 2j6b).

Carton representation of the protein 2j6b is shown in Fig. 8 on the left, together with a schematic structure of a slipknot, as well as a knot obtained after cutting 9 amino acids from the terminal C. 2j6b consists of N=109 amino acids and belongs to α class. It is built of five strands which form the sheet surrounded by a loop from one side and the helix 3-5 on the other side. The secondary structure notation which we use is as follow: 1 – strand (amino acid 2-5); 2 – strand (19-25); 3 – helix (26-37); 4 – strand (39-41);

5 – helix (45-57); 6 – strand (74-80); 7 – helix (92-100); 8 – strand (101-109). The function of AFV3-109 is not known, however it was suggested that it could interact with nucleic acids [17].

A thymidine kinase (PDB code 1p6x) belongs to α class protein and is shown in Fig. 8 on the right. It can be divided into 11 parts denoted by numbers from 1 to 11 in the main text, which are specified as follows: 1 – N terminal with the strand (amino acid 20-34); 2 – helix with turn (35-45); 3 – hairpin and turn (55-60); 4 – big long loop created of 3 helices form one side and closed from the other side by loop 4* (120-132) all together (61-132); 5 – strand (133-139); 6 – hairpin built of two helices (141-176); 7 – strand (177-184); 8 – bundle of five helices (185-299); 9 – strand (300-306); 10 – helix and hairpin (306-323); 11 – the chain crossing the loop 4* (324-333); 12 – helix on the second side of the loop 4 (334-352). The strands 1, 3 and 5 create a characteristic β -sheet. Using this notation for the elements of the secondary structure we identified the following contacts: 1-2, 1-4, 1-4*, 1-5, 1-7, 1-10, 1-11b, 2-3, 2-10, 3-5, 3-10, 3-12, 4, 4-5, 4-6, 4-8, 4-10, 4-11, 4-12, 5-12, 6, 6-8, 7-9, 7-10, 8, 9-10. This list is used to analyze the folding routes and the backtracking between various groups of contacts. Our analysis is mostly concentrated on the loop 4* through which the strand 1, strand 10, and helix 11 have to pass.

B Reidemeister moves

Three Reidemeister moves I, II and III are shown in figure 9. They describe, after a projection on a plane, basic geometric transformations which do not change a topology of a knot. In each move the relative location of the ends of all the strings involved is unchanged. The move I is a transformation of a straight piece of a string into a loop. The move II corresponds to transforming two parallel strings into a configuration with two crossings. The move III involves three strings, and corresponds to a shift of one of them over the crossing made by the other two. These Reidemeister moves are very useful in a simplified description of proteins with nontrivial topology.

C Video clips of folding trajectories for knots and slip-knots

We enclose a video presentations of the mechanism of knot formation, generated using our implementation of the Go-like model. The first animation presents protein 1j85, and the second the protein 1o6d. The process of the knot formation in these animations corresponds to Fig. 1 in the main text. The knotted regions of both proteins are shown by green color. Furthermore, we also enclose a video presentations of the mechanism of slipknot formation in our model, respectively for 2j6b and then 1p6x.

D The intermediate slipknot and the fraction of native contacts for 1o6d

In Fig. 10 the fraction of native contacts Q is shown at the moment when the slipknot is being created, i.e. when its hook-part starts to be threaded through the loop 66-96. In the main trajectory the structure elements located closer to the N terminal of the protein fold in last stages of folding process. These trajectories are represented by red dots and in this case $Q \approx 0.8$. In the second type of trajectories, represented by blue dots, the N terminal folds in initial stages of the folding, and $Q \approx 0.6$. One additional point in the figure represents a very rare knot formation, corresponding to threading the terminus C through the loop 66-96 without a slipknot intermediate. The data shown in this figure corresponds to the optimal model considered in the main text and denoted in bold in the table below. However, there is no qualitative difference in the values of Q between this model and the results obtained in the basic model (with the uniform energetic map).

Apart from the protein 1o6d we also checked the folding ability of another member of YbeA family, i.e. protein with PDB code 1vho. Similarly like 1o6d, this new protein can fold to the native state in the model only based on the native contacts. The folding route includes the slipknot transition state, similarly as for 1o6d and 1j85. However for this protein we also observed one trajectory where the C terminal crosses the loop not in a hairpin-like configuration. The probability of creation of a knot for this protein in a simple model is around 0.1%.

E New energetic map for folding knotted protein 1o6d

From the analysis of the behavior (in particular involving the backtracking) of various elements of the knot structure in 1o6d during folding, shown in Fig. 3 in the main text, we constructed a series of models with new energetic maps. These maps are based only on native contacts and differ in strengths of interactions inside the knotted region of a protein. The energetic maps which we considered are shown in table 1, where these groups of contact are listed whose strength was changed. We found a few energetic maps for which the folding ability is highest – they are shown in rows 15, 17 and 20 in the table 1. For these models we increased twice the sampling set, and under such refined statistics we found that folding ability was the best for the model from the row 15, which we call "optimal". It is also possible to construct energetic maps which prevent knot formation completely, for example by increasing the strength of interaction between contacts for which backtracking is observed (such as strands 5, 6 and 9).

F Folding trajectories for slipknots in 1p6x

We present now in more detail four main folding routes shown in Fig. 11 which are briefly discussed in the main text.

The first route is represented by 5 trajectories which we found. Formation of the slipknot is one of the last steps during folding, and it is possible due to backtracking between strands 1-5, 3-5, and contacts between 3-11 and 4-5. The characteristic property of these trajectories is threading of the terminals N and C through the loop 4, which takes place after or almost in the same time when the entire loop 4 establishes contacts with the segment 8. This event, as well as a correlation between threading almost in the same time the elements 1 and 10, makes this trajectory distinct from all others which we observed. From folding scenario for this route we deduce, that almost all native contacts are created before threading appears, apart from the contacts between N terminal and hairpin of C terminal with loop 4. At this state the contacts between 1-4, 1-5, 4-5 and 4-6 have to be broken to open the loop 4 and allow to thread N and C terminals through it. Now a hairpin is created close to the terminal N, which subsequently moves across the loop 4. By temporary breaking and creating the contacts between terminal N and hairpin 10, the entire C terminal is threaded across the loop 4 also in the hairpin conformation.

The second folding route is represented by 2 trajectories. In this case the chain strongly folds from N terminal by a few different nuclei. This causes creation of a sheet from strands 1, 3, 5, entire loop 4 and its contacts with 6 and 8. In such case (no other native structure of protein is yet established) a small backtracking between elements 1-4 and 1-5 allows easily for crossing terminal N in the bend shape through the loop 4 which creates a knot. After that all other elements of the protein fold. The final event is threading the terminal C across the loop 4 as in the first folding route described above.

The third folding route is most distinct from others. A part of the loop 4, loop 6 (made of two helices) and bundle 8 fold in the same time when contacts between 9 and 10 are established, however all nuclei still exist separately. In the next step big nuclei start to rearrange, which results in a creation of a slipknot with the segments 9, 10 and 11 located inside the loop 4. In contrast to all other trajectories, after this step the N terminal starts to fold and makes half of the sheet clamping the C terminal in the loop 4. Now only the end of the terminal N has to be threaded by the loop 4 (as in the route 1), while the terminal C has to go out of the clamp (as in the route 2). These moves are possible due to backtracking between the segments 1-4, 1-5, 4-5, 1-10 and 3-10.

The fourth trajectory is schematically described in the main text, however now we include more details. We remind that in this route almost entire native structure, apart from contacts between the loop 4 and elements 6 and 8, is created before creation of a slipknot. This conformation corresponds to almost entirely created sheet (involving the elements 1, 3 and 5) with strands 1 and 10 located close to their native positions (as in the knot or slipknot configuration). The final stages of knotting are accompanied by a

backtracking, as shown in Fig. 6 in the main text. We discuss it starting from the moment when the loop 4 is still above the sheet 1-3-5. From this moment the contacts between strands 3-5, helix 2 and strand 3, and a few others, perform amazing backtracking which leads to the rotation of the loop 4 by almost 360 degrees. During this rotation the values of RMSD and RG steadily grow. The contacts inside loop 4 break temporarily in order to provide enough space to accommodate both terminals N and C, which are subsequently threaded through the loop.

Some deviation of the second folding route is represented by two other trajectories, for which the critical role is also played by closing the loop 4. In this case the sheet 1-3-5 is created after establishing entire remaining native structure and before closing the loop 4 (as also described above). This allows for reopening the contacts in sheet and rotation of loop 4 to make the knot, despite somewhat awkward position of the terminal C. In consequence closing of the loop 4 clamps the terminal C between this loop and the sheet for a long time.

Acknowledgments

We appreciate discussions with M. Cieplak, P. A. Jennings, P. Szymczak, and P. Wolynes. We thank D. Gront for help with reconstructing the proteins. This work was supported by the Center for Theoretical Biological Physics sponsored by the NSF (Grant PHY-0822283) with additional support from NSF- MCB-0543906. P. Sułkowski highly appreciates the support of the Humboldt Fellowship and great hospitality of the University of California San Diego.

References

- [1] J. D. Bryngelson, J. N. Onuchic and P. G. Wolynes. Funnels, Pathways, And The Energy Landscape Of Protein-Folding - A Synthesis. *Prot. Stru. Fun. and Gene.*, 21: 167-195, 1995
- [2] H. Nymeyer, N. D. Socci, and J.N. Onuchic Landscape approaches for determining the ensemble of folding transition states: Success and failure hinge on the degree of frustration. *Proc. Natl. Acad. Sci. (USA)* 97:634–639, 2000
- [3] J.N. Onuchic and P. G. Wolynes Theory of protein folding *Curr. Opin. Struct. Biol.* 14(1): 70-75, 2004
- [4] W. R. Taylor. A deeply knotted protein structure and how it might fold. *Nature*, 406:916–919, 2000.

- [5] P. Virnau, L. A. Mirny, and M. Kardar. Intricate knots in proteins: Function and evolution. *PLOS Comput. Biol.*, 2:1074–1079, 2006.
- [6] W. R. Taylor. Protein knots and fold complexity: Some new twists. *Computational Biology and Chemistry*, 31:151–162, 2007.
- [7] N. P. King, E. O. Yeates, and T. O. Yeates. Identification of rare slipknots in proteins and their implications for stability and folding. *J. Mol. Biol.*, 373:153–166, 2007.
- [8] A.L. Mallam and S.E. Jackson. Probing nature’s knots: The folding pathway of a knotted homodimeric protein. *J. Mol. Biol.*, 359:1420–1436, 2006.
- [9] A.L. Mallam and S.E. Jackson. Folding studies on a knotted protein. *J. Mol. Biol.*, 346:1409–1421, 2004.
- [10] A. L. Mallam and S. E. Jackson. Comparison of the folding of two knotted proteins: YbeA and Yibk. *J. Mol. Biol.*, 366:650–665, 2007.
- [11] A. L. Mallam and S. E. Jackson. The dimerization of an β -knotted protein is essential for structure and function. *Structure*, 15:111–122, 2007.
- [12] A. L. Mallam, S. C. Onuoha, J. G. Grossmann and S. E. Jackson. Knotted Fusion Proteins Reveal Unexpected Possibilities in Protein Folding. *Mol. Cell*, 30:642–648, 2008.
- [13] A. L. Mallam, E. R. Morris and S. E. Jackson. Exploring knotting mechanisms in protein folding. *PNAS*, 105:18740–18745, 2008.
- [14] D. Gront, S. Kmieciak, and A. Kolinski. Backbone building from quadrilaterals, a fast and accurate algorithm for protein backbone reconstruction from alpha carbon coordinates. *J. Comput. Chemistry*, 28:1593–1597, 2007.
- [15] D. Gront and A. Kolinski. Utility library for structural bioinformatics. *Bioinformatics*, 24:584 – 585, 2008.
- [16] A. Gardberg, L. Shuvalova, C. Monnerjahn, M. Konrad and A. Lavie. Structural basis for the dual thymidine and thymidylate kinase activity of herpes thymidine kinases. *Structure*, 11:1256–1277, 2003.
- [17] J. Keller, N. Leulliot, C. Cambillau and V. Camapanacci, S. Porciero and D. Prangishvilli. Crystal structure of AFV3-109 a highly conserved protein from cre-narchaeal viruses. *Virol. J.*, 4: 12, 2007.

- [18] C. Clementi and H. Nymeyer and J. N. Onuchic. Topological and energetic factors: what determines the structural details of the transition state ensemble and “on-route” intermediates for protein folding? An investigation for small globular proteins *J. Mol. Biol.*, 298: 937—953, 2000.
- [19] M. Cieplak and T. X. Hoang. Universality classes in folding times of proteins. *Biophys. J.*, 84:475, 2003.
- [20] T. Norcross and T. O. Yeates. A Framework for Describing Topological Frustration in Models of Protein Folding. *J. Mol. Biol.*, 362: 605-621, 2006.
- [21] S. Gosavi, L. L. Chavez, P. A. Jennings and J. N. Onuchic. Topological Frustration and the Folding of Interleukin-1beta. *J. Mol. Biol.*, 357:986—996, 2006.
- [22] S. Wallin, K. B. Zeldovich, and E. I. Shakhnovich. The folding mechanics of a knotted protein. *J. Mol. Biol.*, 368:884–893, 2007.
- [23] J. I. Sułkowska, P. Sulkowski, P. Szymczak and M. Cieplak. How knots influence properties of proteins. *Proc. Natl. Acad. Sci. (USA)*, in print 2008.
- [24] P. Virnau, L. A. Mirny and M. Kardar. Knots in globule and coil phases of a medal polyethylene. *J. Am. Chem. Soc.*, 27:15102-15106, 2005.
- [25] D. M. Raymer and D. E. Smith. Spontaneous knotting of an agitated string. *Proc. Natl. Acad. Sci. (USA)*, 104:16432-16437, 2007.
- [26] J. I. Sułkowska, P. Sulkowski, P. Szymczak, and M. Cieplak. Tightening of knots in the proteins. *Phys. Rev. Lett.*, 100:58106, 2008.
- [27] M. Cieplak, T. X. Hoang, and M. O. Robbins. Thermal effects in stretching of go-like models of titin and secondary structures. *Proteins: Struct. Funct. Bio.*, 56:285–297, 2004.
- [28] M. Cieplak, T. X. Hoang, and M. O. Robbins. Stretching of proteins in the entropic limit. *Phys. Rev. E.*, 69:011912, 2004.
- [29] S. Gosavi and P. C. Whitford and P. A. Jennings and J. N. Onuchic. Extracting function from a β -trefoil folding motif *Proc. Natl. Acad. Sci. (USA)*. in press, 2008.
- [30] J. I. Sułkowska and M. Cieplak. Selection of the optimal variants of go-like models of proteins through studies of stretching. *Biophys. J.*, 95:3174—3191, 2008
- [31] N. D. Socci, J. N. Onuchic and P. G. Wolynes. Stretching lattice models of protein folding. *Proc. Natl. Acad. Sci. (USA)*., 96:2031–2035, 1999.

- [32] H. X. Zhou. Loops, linkages, rings, catenanes, cages, and crowders: entropy-based strategies for stabilizing proteins. *Acc. Chem. Res.*, 37:123–130, 2004.
- [33] K. Koniaris and M. Muthukumar. Knottedness in ring polymers. *Phys. Rev. Lett.*, 66:2211–2214, 1991.
- [34] P. Szymczak and M. Cieplak. Influence of hydrodynamic interactions on mechanical unfolding of proteins. *J. Phys. Cond. Mat.* 19:258224, 2007

Table 1:

Order	region*	region*	region*	region*	success rate
1.	5-8*0.5				3
2.	5-8*2				9
3.	5-8*4				10
4.	5-8*6				9
5.	5-8*10				1
6.	5-8*2	6-10*2			15
7.	5-8*4	6-10*2			9
8.	5-8*10	6-10*2			12
9.	5-8*2	6-10*4			14
10.	5-8*2	6-10*6			8
11.	5-8*2.5	6-10*2.5			6
12.	5-8*2		(7-10,8-10,9-10)*0.5		2
13.	5-8*2		(7-10,8-10,9-10)*1.5		2
14.	5-8*2	6-10*2	(7-10,8-10,9-10)*0.5		25
15.	5-8*2	6-10*2	(7-10,8-10,9-10)*0.5	without 74-115	34
17.	5-8*2.5	6-10*1.5	(7-10,8-10,9-10)*0.5	without 74-115	25
18.	5-8*2	6-10*3	(7-10,8-10,9-10)*0.5	without 74-115	27
19.	5-8*1	6-10*3	(7-10,8-10,9-10)*0.5	without 74-115	15
20.	5-8*2	6-10*2	(7-10,8-10,9-10)*0.5	turns*2	34
21.	5-8*2			5-9*2	3
22.	5-8*2			6-9*2	2

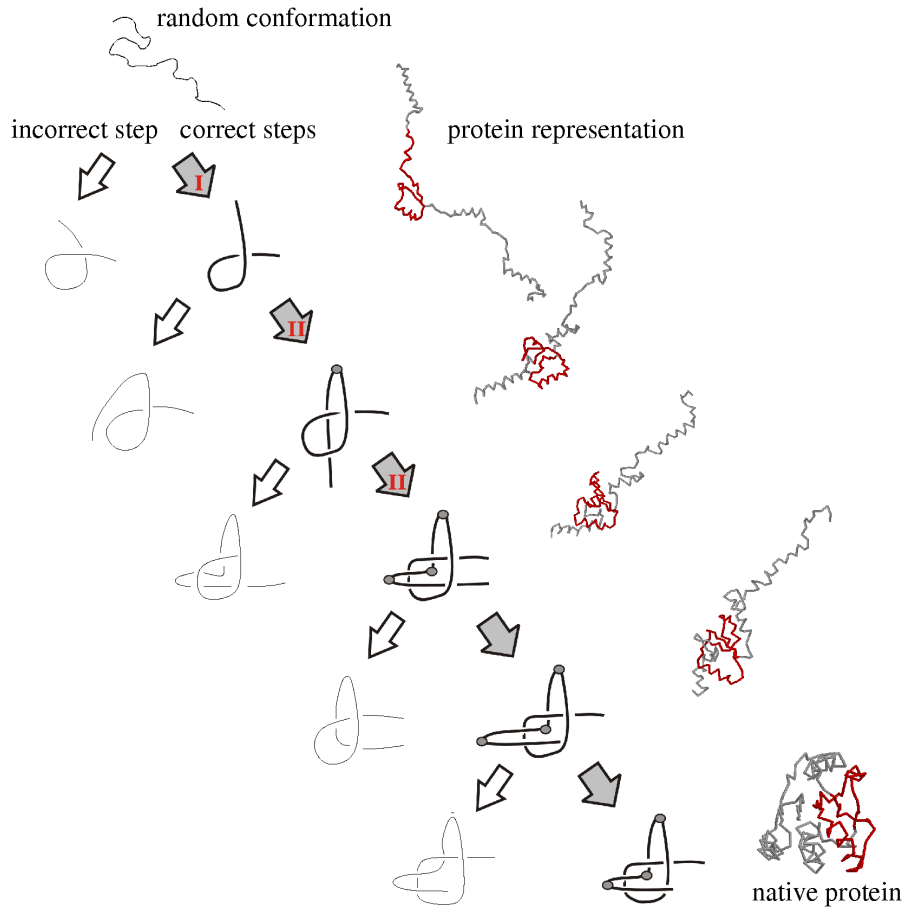


Figure 2: The folding route that leads to the native knotted configuration 3_1 through an intermediate configuration with a slipknot. The pathway is represented by a series of configurations, starting in the top left (a random conformation) and proceeding towards the right bottom. The path involves five essential steps, the first three of them correspond to the Reidemeister moves I and II (denoted on appropriate arrows). A typical representation of the protein conformations are shown to the right of the associated mechanistic step. Native-like locations of the knot are shown in red. Each step is characterized by the appearance of new structural elements such as loops and hooks. During the folding route incorrect steps may occur. Examples of some incorrect configurations, which are kinetic traps, are represented by thin lines (sketched on the left). These traps act as topological barriers [20] and escaping from them requires a backtracking mechanism similar to the ones we have observed in regular folding [21]. Grey dots represent amino acid 102 in the third step plus amino acids 114 and 124 in the following steps. Special emphasis is given to them since they are associated to sharp turns, which are required to achieve the knotted state. This folding process is shown in the attached movie, whose details are described in *Appendix*.

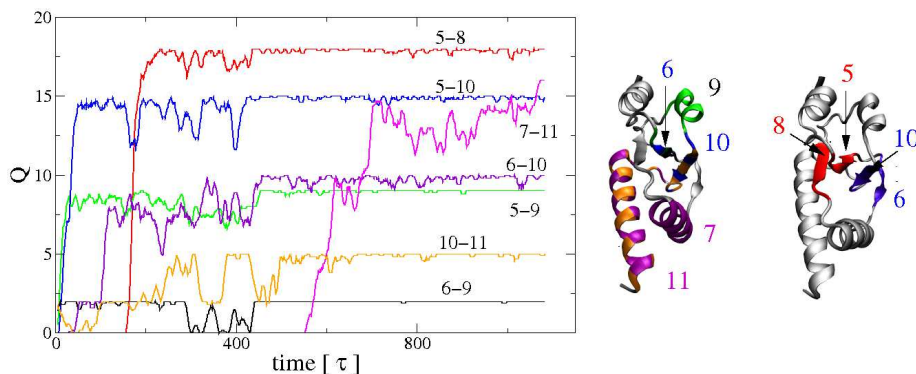


Figure 3: Left: the time dependence of the number of formed native contacts between relevant structural elements of the protein knot, 1od6. Right: cartons representation of knotted part of the protein 1od6. Interacting regions of the protein 1o6d are colored accordingly to the ones used in each trajectory. For clarity, if there are native interactions of one secondary structure element with two different parts of the protein, they are shown on two separate structures. Backtracking is observed at different levels for all trajectories. The contacts between strands 5-8 are colored red, the ones between strands 6-10 are magenta, and the ones for the turn 97-105 are orange. Kinetic studies were performed using overdamped Langevin dynamics. Timesteps have been chosen to have typical folding times of about 1000 steps.

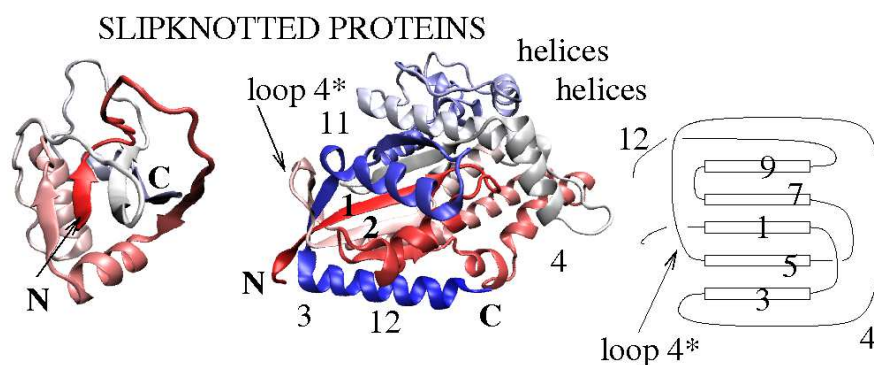


Figure 4: Structure of two proteins with slipknots: crenarchaeal viruses AFV3-109 (2j6b) (left) and a thymidine kinase (1p6x) (middle). Right: a schematic representation of the structure of 1p6x. Stereo-views of proteins is shown in the Appendix.

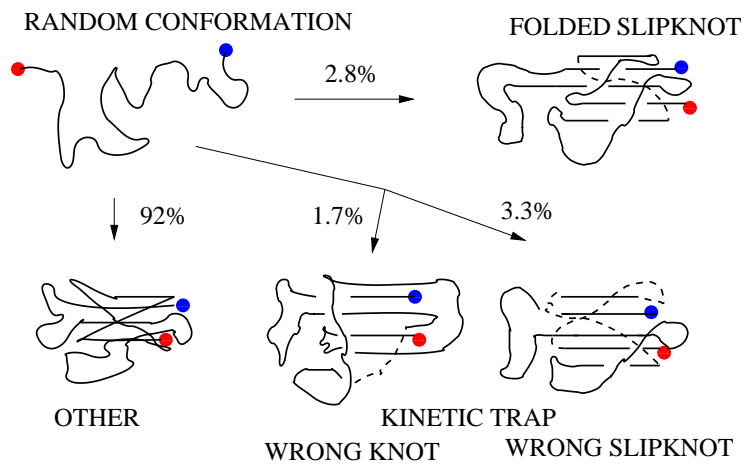


Figure 5: Schematic representation of the four different ensembles of final conformations observed in 1000 folding runs of the slipknotted protein 2j6b. Simulations were performed at temperatures slightly above T_f . Only the structure in the top right corresponds to the correctly folded protein with the correct slipknot and all native contacts.

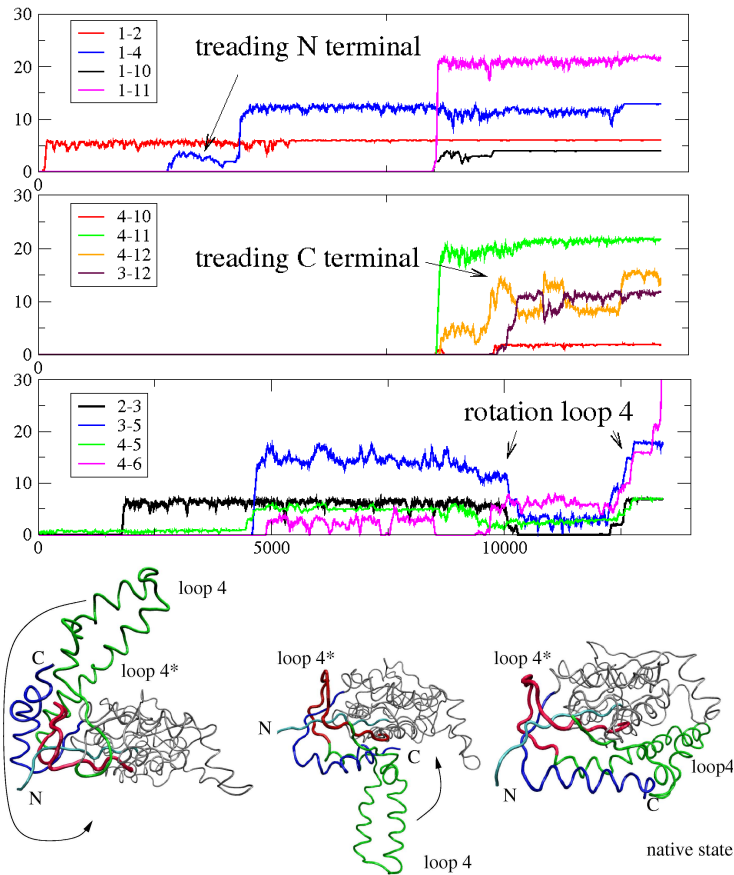


Figure 6: The folding route for 1p6x (described as the fourth one in the text) which involves a rotation of the loop 4. The three figures from the top, respectively: average number of contacts in indicated sets of secondary structure around N terminal, C terminal and loop 4 during the folding of 1p6x. Bottom panel: steps which leads to a formation of a knot and slipknot structure by the rotation of the loop 4. The steps are connected to the top panels in the following way. In the first panel at time 2000 the knot is already partially formed, but not yet a slipknot, thus the loop 4 is still above the sheet 1-3-5. Then the backtracking follows, which involves strands 3-5, helix 2 and strand 3, and a few others, as seen in the second panel. During the rotation of this loop values of RMSD and RG steadily grow. The contacts inside loop 4 break temporarily to provide sufficient space to accommodate N and C terminal, which are subsequently threaded through this loop, and which eventually leads to a slipknot conformation. The colors of various elements of the structure in the bottom panel match corresponding contact numbers in the top panel. This folding process is shown in the attached movie, whose details are described in *Appendix*.

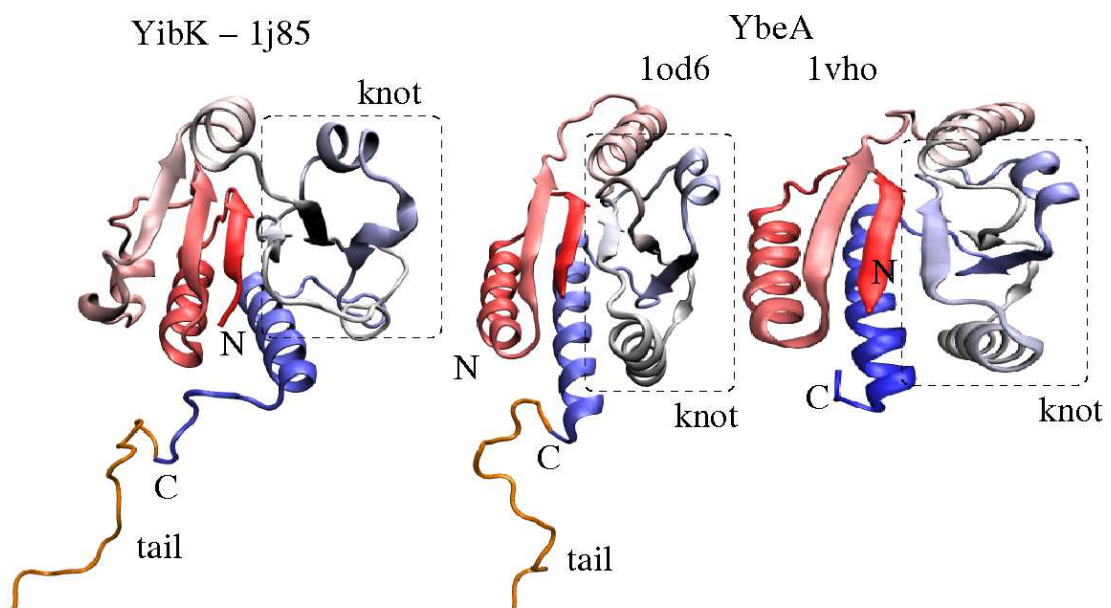


Figure 7: Left: 1j85. Middle: 1o6d. Right: 1vho. For each protein a region where the knot is localized is denoted by a dashed rectangle.

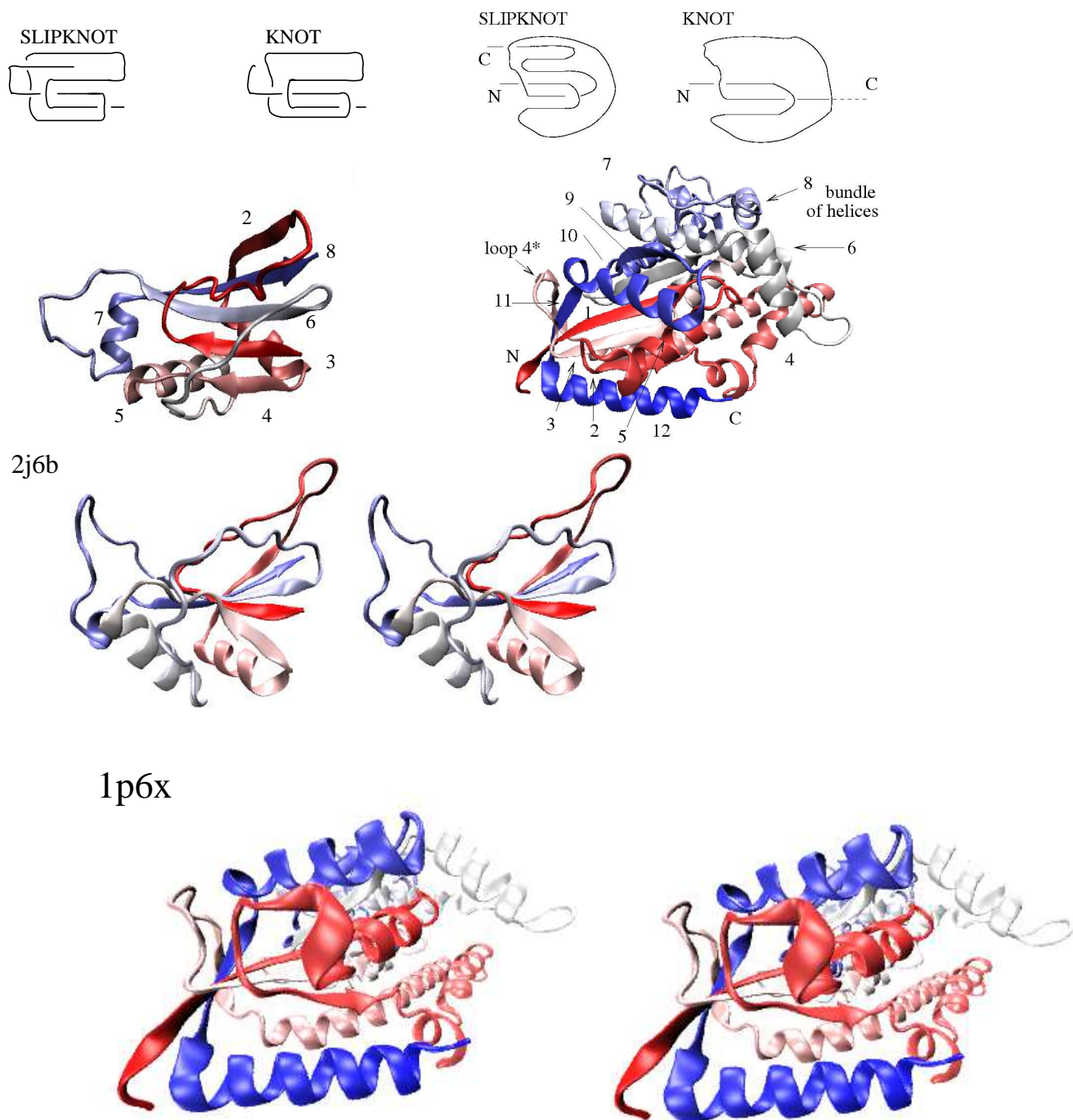


Figure 8: Bottom: cartoon structures of proteins 2j6b (left) and 1p6x(right) . Top: the corresponding schematic structures of a slipknot in these proteins, as well as the knotted conformation 3_1 obtained after cutting, respectively, 20 amino acids from the N terminal (for 2j6b), or a few amino acids from C terminal (for 1p6x). The lowest figures stereoview of proteins 2j6b and 1p6x.

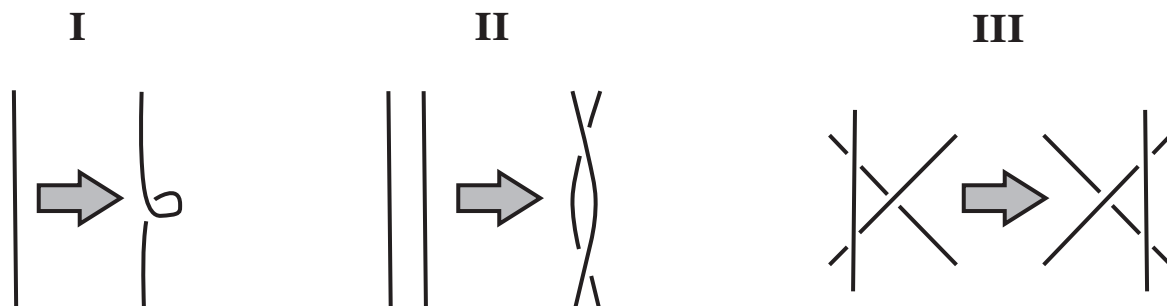


Figure 9: Reidemeister moves I, II and III.

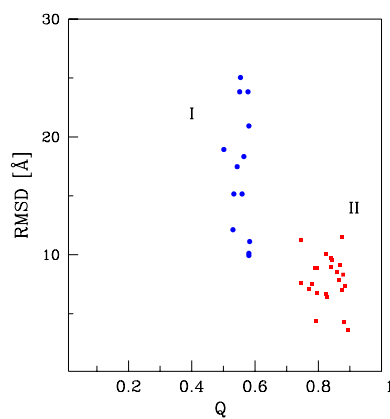


Figure 10: Distribution of native contacts in protein 1o6d at the moment when slipknot configuration appears for the first time during folding. This moment corresponds to the fourth step in Fig. 2 in the main text. The results are similar both for the model with the optimal native like energy scale, and the basic model with uniform energy. The symbol I corresponds to folding from the terminal C, while II to folding from terminal N.

